Interlevel Ge/Si quantum dot infrared photodetector

A. I. Yakimov,[a] A. V. Dvurechenskii, A. I. Nikiforov, and Yu. Yu. Proskuryakov
Institute of Semiconductor Physics, Siberian Branch of the Russian Academy of Sciences, 630090 Novosibirsk, Russia

(Received 27 April 2000; accepted for publication 7 December 2000)

A self-assembled Ge/Si quantum dot interlevel infrared photodetector operating at room temperature and at normal incidence is demonstrated. The spectral response exhibits two peaks in the 58–82 and 132–147 meV energy regions with full width at half maximum linewidths as narrow as 25 meV. The two photocurrent maxima are ascribed to transitions from the hole ground state to the excited states in the dots. The peak detectivity and responsive quantum efficiency are 1.7×10^{8} cm $Hz^{1/2}$/W and 0.1% for the transition from the ground state to the first excited state and 7×10^{7} cm $Hz^{1/2}$/W and 0.08% for the transition from the ground state to the second excited state. At large dc bias, a redshift in the transition energies is observed. We argue that the resonance shifts are due to suppression of the depolarization field effect, representing the experimental manifestation of dynamic screening associated with collective electron–electron interaction in the dots. © *2001 American Institute of Physics.* [DOI: 10.1063/1.1346651]

I. INTRODUCTION

Intersubband transitions in quantum well system involve the absorption of a photon to cause an electron to be transferred from one confined state to a higher confined state in the well. In quantum dots (QDs), the interlevel transitions are the subject of interest both for their fundamental physics and for development of infrared photodetectors and lasers. With quantum wells, the additional in-plane confinement of carriers and the discrete energy spectrum lead to attractive properties in the infrared region.[1] The potential advantages of QDs for such applications as compared with two-dimensional systems are (i) predicted reduction of the relaxation rates between the confined states[2] leading to increased detection efficiency, and (ii) increased sensitivity to normally incident photoexcitation as a result of breaking of the polarization selection rules, so eliminating the need for reflectors or gratings.

The detection of long-wavelength infrared radiation with $\lambda\simeq10$ μm requires a small gap ($E_g\simeq0.1$ eV) semiconductor. HgCdTe detectors are commonly used for this purpose due to their high responsivity. Compared with HgCdTe-based devices, quantum dot photodetectors are expected to have several advantages such as possible fabrication of large-area low-cost arrays in which the band structure and spectral response can be controlled accurately.

Following successful growth of arrays of high quality QDs by the coherent Stranskii–Krastanov growth method, there has been much interest in exploring the possibility of using interlevel absorption in them for long wavelength infrared photodetectors. To date, most of the work in this field has concentrated on the InAs/GaAs QDs.[3–11] In particular, photoconductivity signals peaking at 17 μm[6] and at 13 μm[7] have been observed in InAs/GaAs QDs for normal incidence illumination at $T=90$ and 40 K, respectively. Cho *et al.*[5] have demonstrated an InAs/GaAs infrared photodetector operating at room temperature. The spectral response has a peak at 10.6 μm with detectivity $D^*=3\times10^{7}$ cm $Hz^{1/2}$/W.[5] Strong normal incidence absorption (7.8% at 77 K and ~3% at 300 K) in the 10.6–20 μm wavelength region has been observed for ten layers of InAs/InAlAs QDs grown on InP(001) substrates.[12] The oscillator strength of the intersubband transition was comparable to that achieved in quantum wells. Johnson noise limited detectivity of 1.33×10^{9} cm $Hz^{1/2}$/W at 10.3 μm and 78 K has been reported for InAs/GaSb QDs superlattices also at normal incidence.[13]

Optical properties of Ge/Si QDs are less studied. Liu *et al.*[14,15] have observed interlevel absorption for radiation polarized along the growth direction in boron doped Ge quantum dots. An in-plane polarized intraband transition (4.2 μm wavelength) in the valence band of Ge QDs, characterized by a huge absorption cross section, 3×10^{-13} cm^2, has been detected by photoinduced infrared spectroscopy.[16] Photocurrent response around 4 μm in normal incidence geometry has also been observed by Miesner *et al.*[17] Recently, we have reported on normal-incidence infrared photoconductivity in Si *p-i-n* diode with embedded Ge QDs.[18] The two kinds of absorption observed in the midinfrared range, which show opposite response to reverse bias, have been ascribed to the intraband hole bound-to-continuum transition and to the interband excitonic transition. The ionization energy of the hole ground state in the dots with respect to the Si valence band (onset of the photocurrent), E_0^i, has been found to be ≈400 meV. Here we study the intersublevel transitions in modulation-doped Ge/Si dot multilayer structures. The large areal density of the QDs ($\sim3\times10^{11}$ cm^{-2}) allowed us not only to achieve the high detector performance in the long-wavelength (9–25 μm) region at room temperature but also to observe collective intersubband excitation effects resulting from interactions between the quantum dots.

[a]Electronic mail: yakimov@isp.nsc.ru

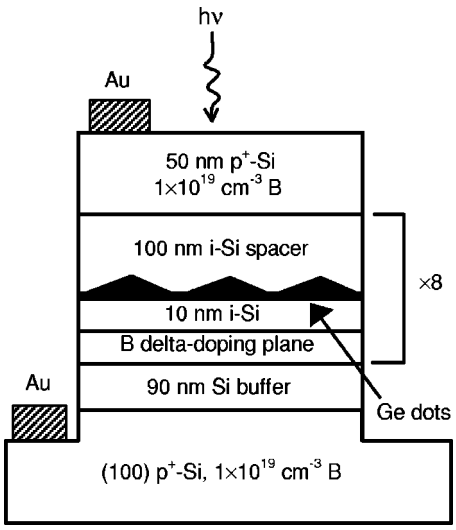

FIG. 1. Schematic of the device structure with self-assembled Ge quantum dots.

II. EXPERIMENTAL DETAILS

Figure 1 shows schematically the detector structure. The sample was grown by solid source molecular beam epitaxy on a (001) oriented 0.01 Ω cm boron doped Si substrate. It composed of eight stacks of Ge quantum dots separated by 110 nm Si barriers. Each Si barrier contains a boron delta-doping layer inserted 10 nm below the Ge wetting layer to produce, after spatial transfer, a 6×10^{11} cm^{-2} hole concentration in the dots corresponding to complete filling of the dot ground state. Each Ge QD layer consisted of a nominal Ge thickness of 10 ML (~14 Å) and was grown at 300 °C at a growth rate of 0.2 ML/s. The Si barriers were grown at 500 °C with temperature ramps before and after QD growth. The buffer Si layer was grown at 800 °C at 2 ML/s.

The growth of the Ge layers was monitored by reflection high-energy electron diffraction where the transition from two-dimensional to three-dimensional island growth was observed after ~5 ML of Ge deposition. Transmission electron microscopy and scanning tunneling microscopy showed that the dots have a pyramid shape with a typical base length of 15 nm and height of 1.5 nm.[18] As stated before, the area density of the dots is estimated to be 3×10^{11} cm^{-2}.[18] Finally, a 50-nm-thick Si contact layer ($p=10^{19}$ cm^{-3}) was deposited. The device was fabricated in a conventional quantum well infrared photodetector configuration, i.e., a mesa structure with vertical contacts on the bottom and top of the structure (Fig. 1). The mesas were 1.5×1.5 mm^2 with Au pads 0.5 mm in diameter.

The photocurrent spectra of the device were measured in a single-pass normal incidence geometry at room temperature. Unpolarized light from a globar source was chopped mechanically at a frequency of about 500 Hz and illuminated on the front side of the detector after passing through a monochromator. A 5 kΩ series resistor was used to convert the photocurrent signal to a voltage signal which was measured using an amplifier and a lock-in detector. In order to obtain the responsivity of the QD detector, the spectral photon flux from the light source was measured by using a calibrated pyroelectric detector. To reduce the signal to noise ratio, the photoresponse at each applied bias was obtained by averaging measurements over several hours.

III. RESULTS AND DISCUSSION

A. Dark current measurements

A typical detector room temperature differential resistance was ~4 kΩ at zero voltage corresponding to an effective ''resistivity'' of about 10^6 Ω cm, which is larger than that of intrinsic silicon, 2.3×10^5 Ω cm. This means that (i) there is band bending around the dot layers due to formation of depletion regions and (ii) carriers are localized deep in the dots, not participating in conduction. In this situation the dominant transport mechanism is expected to be by hole injection from the contacts into the Si valence band. From the measured capacitance of the sample, $C=6.7\times10^{-8}$ F/cm^2, we calculate the total width of the depletion region to be 150 nm (i.e., ≈19 nm per layer of QDs). Although this value is smaller than the distance between top and bottom electrodes, the depletion layers still cause a large increase in the sample resistance. Application of a voltage of ~1 V to the capacitor-like structure with $C=6.7\times10^{-8}$ F/cm^2 results in injection into the sample of a charge density of $\sim4\times10^{11}$ cm^{-2}, which is comparable with the density of quantum dots. As we will see later, this extra charge is captured by the empty states of the QDs and can affect significantly the photodetector performance.

The space-charge limited current in the presence of initially empty traps is given by[19]

$$I_d=\theta\frac{9\epsilon_0\epsilon\mu A}{8L^3}V^2, \tag{1}$$

where A is the sample area, ϵ is the dielectric constant, μ is the carrier mobility, and L is the sample length. The parameter θ characterizes the ratio between injected and trapped carrier concentrations and is given by[19]

$$\theta=\frac{N_vL_p}{gn_t}\exp[-E_t/kT], \tag{2}$$

where N_v is the effective density of states in the Si valence band, g is the level degeneracy, n_t is the areal trap concentration (converted into an average three-dimensional density by dividing by the superlattice period L_p), and E_t is the energy of trap. Dark current versus bias voltage is shown in Fig. 2. At low voltage ohmic behavior is observed implying a low injection level. At $V>0.1$ V, $I_d\propto V^2$, which is a characteristic feature of the space-charge limited current.

From Eqs. (1) and (2) we can derive E_t. For $\theta=10^{-3}$ (determined from the slope of the current–voltage characteristic), $g=4$,[20,21] $\epsilon=11.7$, $L\approx1$ μm, $L_p=110$ nm, $\mu=150$ $cm^2/V\,s$ (determined by Hall measurements), $n_t=3\times10^{11}$ cm^{-2}, we obtain $E_t=298$ meV which is close to the ionization energy of the first excited state in the Ge dots E_1^i ≈290 meV.[20] Correcting expression (1) for the fact that charge is injected only into the depletion layer, we find E_t ≈320 meV.

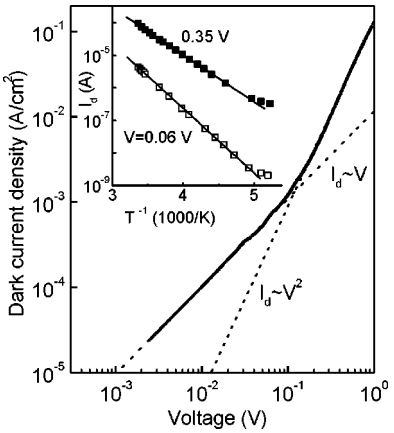

FIG. 2. The dark-current voltage characteristics measured at room temperature. The inset shows the dark current measured at $V=0.06$ V and at $V=0.35$ V plotted as functions of inverse temperature.

Filling of the excited state with increasing bias voltage is further confirmed by measurements of the sample resistance at different temperatures. In the inset of Fig. 2, the dark currents measured in the ohmic regime (at $V=0.06$ V) and in a regime of space-charge limited current (at $V=0.35$ V) are plotted as functions of inverse temperature. At $T>200$ K, the current increases exponentially with T, showing a clear activated behavior. The activation energies were determined to be 405 meV at the lower V and 302 meV at the higher V. The former value is consistent with the ionization energy of the ground state in the dots, E_0^i, while the latter is again close to E_1^i. From these we obtain the separation of the ground and the first excited state in the dots as the difference between E_0^i and $E_t \equiv E_1^i$. The result is about 100 meV which is in reasonable agreement with that obtained previously in field-effect measurements[21] (122 meV) . One has to remember that since the excited state captures *extra* holes, this energy includes both the quantum energy E_{01} and the correlation (charging) energy. In such small dots the latter can be comparable in magnitude with the former.[21,22]

The dark current noise i_n versus positive bias voltage is depicted in Fig. 3(a). The data for negative voltage are very similar. The optical gain g_{opt} can now be obtained using the photoconductor current shot-noise expression[23]

$$i_n = \sqrt{4eI_d g_{\text{opt}} \Delta f}, \tag{3}$$

where Δf is the bandwidth. Combining i_n from Fig. 3(a) and I_d allows the experimental determination of g_{opt} as shown in Fig. 3(a) (right scale). Usually the optical gain increases linearly with bias at low voltage and saturates at high voltage (due to velocity saturation). For the detector under investigation, one sees quite different behavior. The initial increase of g_{opt} is due to the usual increase in velocity with field. However, at $V>0.1$ V, g_{opt} starts to decrease strongly tending to unity. This means that once a carrier excited from a dot leaves the sample another one is immediately injected into the dot, thereby increasing the dot capture probability and reducing recapture lifetime. From $\tau_r = L^2 g_{\text{opt}}/\mu V$ we can infer the hot-carrier transport recapture lifetime τ_r as shown in Fig. 3(b).

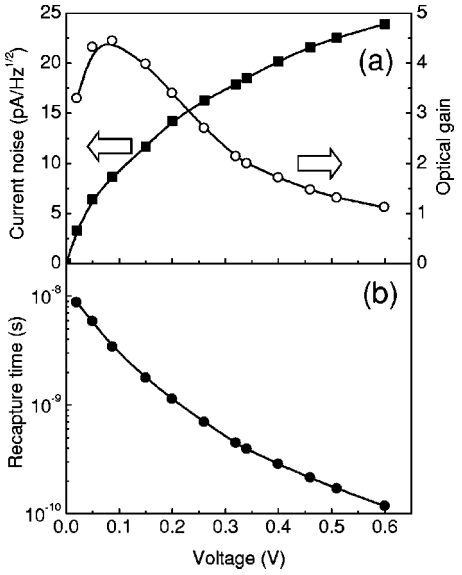

FIG. 3. Dark current noise and optical gain (a), and recapture lifetime (b) vs bias voltage. The solid lines are guides to the eye.

B. Responsivity and detectivity

Figure 4 shows the room temperature responsivity spectrum measured at different bias voltages. Two distinct transitions dependent on the applied voltage and polarized parallel to the layers are observed. One peaks in the range 58–83 meV and the other between 132–147 meV. The full width at half maximum of about 25 meV is considerably smaller than that for bound-to-continuum transitions observed in a Ge/Si quantum dot photodiode ($\sim$150 meV).[18]

As stated before, the chosen doping concentration was design to populate the QDs ground state only. Only transitions from this state are expected to be observed. We attribute the two absorption peaks to the excitation of holes from the ground state, E_0, to the first excited state E_1 (E_{01} transition) and to the second excited state E_2 (E_{02} transition) in the dots as shown in Fig. 4. After absorption of the infra-

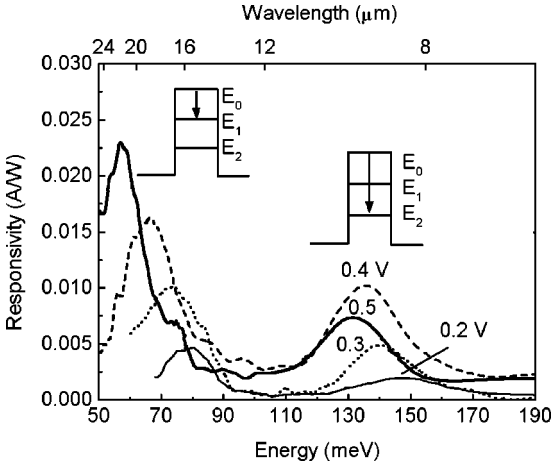

FIG. 4. Photoconductive spectral response of the quantum dot photodetector at various bias voltages. E_0 is the energy of the hole ground state in the dots, and E_1 and E_2 are the energies of the first and second excited states of holes, respectively.

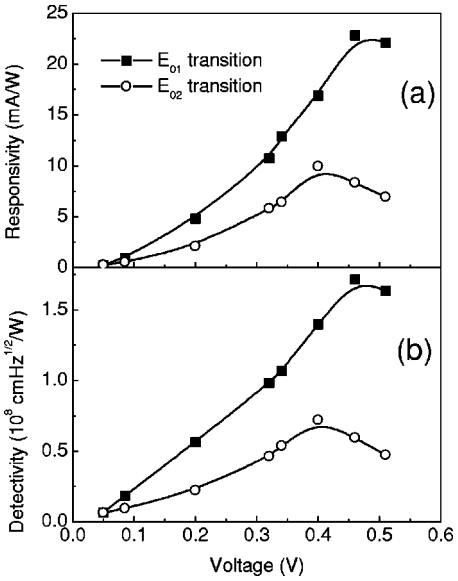

FIG. 5. Peak responsivities (a) and detectivities (b) as functions of applied voltage. The solid lines are guides to the eye.

red photon, the photoexcited hole can escape from the state E_1 or E_2 by thermoionic emission over the barriers to the continuum transport states, and be collected as photocurrent. The measured energy spacing is in a reasonable agreement with resonant tunneling experiments,[22] where the E_{01} was found to be ≈ 75 meV and the E_{02} was about 140 meV. Some deviation could arise from the fact that the present dots are modulation doped, and thus, the energy spectrum is affected by the charged impurities in the delta-doping planes. Another possible explanation is that residual vertical correlation between islands in successive layers might cause the size of the dots in multilayer structures to differ from that in a single layer.[24]

It should be noted that for a symmetric quantum well, the dipole matrix elements of transitions for odd-to-odd or even-to-even quantum numbers vanish since the envelope functions of these states have the same parity. This restriction is removed in asymmetric wells.[25] The absence of rotational symmetry in the Ge QDs (they are rectangular in base) allows the normally forbidden $0 \rightarrow 2$ transition to occur.

We can now calculate the peak detectivity D^* using[26,27]

$$D^* = R\sqrt{A\Delta f}/i_n,$$

where A is the detector area and $\Delta f = 1$ Hz. The responsivity R and detectivity D^* at peak wavelength for various positive bias voltages are depicted in Fig. 5. Under a large bias ($V > 0.4$ V) both R and D^* tend to be reduced due to decrease of the optical gain and accumulation of holes in the excited states, thereby blocking the intersubband transitions and, hence, reducing the absorption strengths. The highest peak detectivity at normal incidence is 1.7×10^8 cm Hz$^{1/2}$/W. This value is about five times larger than that in InAs/GaAs longwave photodetector at the same temperature,[5] and comparable with detectivity of uncooled thermal and pyroelectric detectors.[28] This demonstrates the superiority of Ge/Si QDs detectors for high-temperature operation.

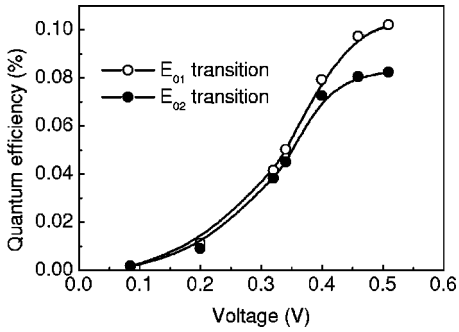

FIG. 6. Quantum efficiency vs bias voltage. The solid lines are guides to the eye.

At $V = 0.5$ V, an additional shoulder at energy of ≈ 75 meV can be seen in the photocurrent spectrum. We attribute this feature to a transition between the first and second excited states (the E_{12} transition). Obviously, the transition energy should be equal to the energy difference between the E_{02} and E_{01} transitions. Taking the experimental values $E_{02} = 132$ meV and $E_{01} = 58$ meV we obtain $E_{12} = 74$ meV which is consistent with the experimental observation.

The detector quantum efficiency η can be found combining the bias-dependent optical gain g_{opt} with the peak responsivity R using the well-known equation[23]

$$R = (e/h\nu)\,\eta g_{\text{opt}}, \tag{4}$$

where $h\nu$ is the photon energy. Results are shown in Fig. 6. As the bias is increased the quantum efficiency increases strongly and then saturates, reaching a maximum value of about 0.1%. One has to remember that the net quantum efficiency is a product of an absorption factor η_a and an escape factor p_e, which characterizes the probability that a photoexcited carrier will escape from the quantum dot and contribute to the photocurrent, rather than being recaptured by the originated dot. Taking $\eta_a \sim 0.003$[29] of ten QD layers, we find that $p_e \approx 0.3 < 1$, which supports our interpretation of the observed photoresponse as being due to the transitions between strongly localized states.

C. Shift of the transitions in electric field

We now turn to discussion of the voltage induced change in the intersubband absorption energy. Apart from the possible practical application of electric modulation in tunable infrared modulators,[30] this effect gives rise to interesting issues relating to collective excitation in arrays of quantum dots. Usually, shifts of the quantum well intersubband transitions in a perpendicular electric field are ascribed to the quantum-confined Stark effect.[31–34] For a symmetrical well the applied field causes an increase in the energy difference $(E_n - E_0)$ due to driving the ground state further into the triangular potential well formed in the bottom of the well.[32] For an asymmetrical well the transition energies can be either blue- or redshifted depending on the direction of the field.[33,34] We find quite different behavior, however: both the $0 \rightarrow 1$ and $0 \rightarrow 2$ transitions exhibit a redshift independent of bias polarity (Fig. 7). The reason why we do not expect any Stark effect in our sample becomes clear from a simple

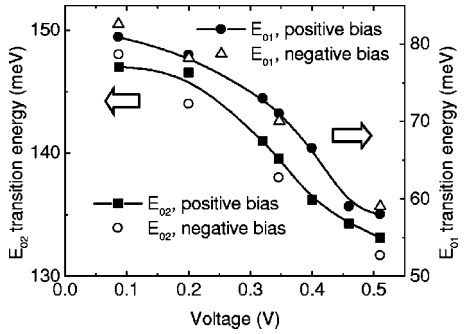

FIG. 7. Shift in transition energies as functions of applied bias of either polarity. The solid lines are guides to the eye.

order-of-magnitude argument. The confinement energies of the first levels are $\approx 50-100$ meV. The wave functions of the holes in the dots have an extent perpendicular to the layers comparable to the dot height (e.g., ≈ 1.5 nm). Consequently, applying fields ≈ 0.5 V/μm (i.e., only 0.75 meV/1.5 nm well) cannot change transition energies by 10–20 meV as seen in Fig. 7. Thus, the Stark effect cannot be responsible for our observations.

A different effect which can become important with increasing population of excited states is direct Coulomb interaction between holes. Dependence of the electronic spectrum on the number of electrons in a dot is a Coulomb-blockade phenomenon.[35] As a result of hole accumulation in excited states of the QDs, the self-consistent Hartree potential will shift all E_i to higher energy. As the wave function overlap is reduced, there is no appreciable Coulomb interaction between holes in the populated ground state and holes in the excited state,[36] although the interaction inside the excited subbands can be significant. Similar arguments are valid for the exchange interaction also.[36] Since the ground state level is affected by static interaction with extra holes much less than the excited state is, there would be an upward shift in the transition energy, the opposite of what we observe.

We attribute the observed shift in Fig. 4 to many-particle interaction effects.[29] In a two-dimensional electron gas, the energies of intersubband excitations are known to be shifted from single-particle subband spacings by two effect associated with dynamic electron–electron interactions. One is a upward shift caused by the collective plasma oscillation,[37–39] also known as the depolarization (or resonant screening) effect. The other is a downward shift arising from exciton-like exchange correlations between optically excited electrons and remaining electrons.[40] Recently, Metzner and Döhler[41] have examined the role of dynamic many-particle effect for the intersubband absorptions in a quasi-two-dimensional electron layer with strong lateral disorder. This system was considered to be equivalent to an array of randomly distributed localized oscillators or quantum dots mutually coupled by electron–electron Coulomb interaction. For such a system, the authors predicted a depolarization-type effect, similar to that observed in convential two dimensional systems.

Previously we have studied the effect of a nearby bulk conductor on hopping transport in similar arrays of Ge QDs.[42] We found that putting a metal plane close to the dot layer causes a crossover from Efros–Shklovskii variable-range hopping conductance to two-dimensional Mott behavior. In the Efros–Shklovskii hopping regime, the conductance prefactor was found to be $\simeq e^2/h$, and conductance scales with temperature. In the fully screened limit, the universal behavior of the prefactor is destroyed and it begins to depend on the localization length. These experimental results were explained in terms of screening of long-range Coulomb interaction and give evidence for strong electron–electron coupling between dots in the absence of screening. It seems to be reasonable to assume that the system under investigation here should also display dynamic interaction effects of this sort.

The physics of the depolarization effect can be understood from the following scenario.[41] Let us consider a planar array of QDs. Initially two holes are in the ground state of each dot and the excited states are assumed to be unoccupied. Normal incidence of infrared radiation implies that an external electric field $\mathcal{E}_{\rm ex}(t)=\mathcal{E}_0 e^{-i\omega t}$ is applied in the direction parallel to the plane of the dots. This field causes resonant transitions of holes between in-plane polarized QD bound states. This corresponds in real space to transverse oscillations of holes within their associated QDs. The oscillating charge density results in a long-range time-dependent Coulomb potential which couples the motion of all holes leading to collective intersublevel excitations. As a result of polarization, the actual field inside the dots is changed and the optical resonance is blueshifted. In other words, the single-particle optical resonances are ''dressed'' by interaction with collective oscillations of the entire hole gas.

Let us return to our experiments. As we demonstrated earlier, under applied bias the level population is changed due to hole injection from the contacts. This situation has been analyzed theoretically by Załużny.[43] His theory predicts the depolarization shift to be a function of the difference in population of the subbands. On biasing, the excited states become occupied. This suppresses the depolarization effect and causes the transition energy to be shifted downward to its single-particle value E_{0i}. Similar redshift of the absorption peak at high intensities of far infrared radiation (FIR) has been observed previously in AlGaAs/GaAs quantum well.[44] Increasing the FIR intensity in Ref. 44 and increasing the bias voltage in our experiments both cause the population in the excited subbands to increase and the collective excitations to be undressed.

IV. CONCLUSION

We report a long-wavelength infrared photodetector based on Ge self-assembled quantum dots and operating at normal incidence. The structure uses intersubband transitions of holes in the dots. The maximum room temperature peak detectivity and quantum efficiency of a nonoptimized device structure at about 20 μm were found to be 1.7×10^8 cm $\mathrm{Hz}^{1/2}$/W and 0.1%, respectively.

The transitions are found to be redshifted strongly with increasing voltage so providing an excellent modulator for 10.6 μm CO_2 laser radiation. We argue that the observed shift in the intersubband transition energies results from suppression of the depolarization effect associated with collec-

tive response in a dense ensemble of interacting quantum dots.

ACKNOWLEDGMENTS

The authors wish to thank John Adkins for very useful discussions. This work was supported by the Russian Foundation of Basic Research (Grant No. 99-02-17019) and by the Russian State Scientific Program on Physics of Solid State Nanostructures (Grant No. 98-1100).

[1] For a brief discussion of the potential of the quantum dot infrared photodetectors, see H. C. Liu, Physica E (Amsterdam) **8**, 170 (2000).
[2] M. Sugawara, K. Mukai, and H. Shoji, Appl. Phys. Lett. **71**, 2791 (1997).
[3] S. Sauvage, P. Boucaude, F. H. Julien, J.-M. Gérard, and V. Thierry-Mieg, Appl. Phys. Lett. **71**, 2785 (1997).
[4] S. Sauvage, P. Boucade, F. H. Julien, J.-M. Gérard, and J.-Y. Martin, J. Appl. Phys. **82**, 3396 (1997).
[5] T. Cho, J.-W. Kim, J.-E. Oh, and S. Hong, Tech. Dig. Int. Electron Devices Meet. **1998**, 441.
[6] J. Phillips, K. Kamath, and P. Bhattacharya, Appl. Phys. Lett. **72**, 2020 (1998).
[7] D. Pan, E. Towe, and S. Kennerly, Appl. Phys. Lett. **73**, 1937 (1998).
[8] S. Maimon, E. Finkman, G. Bahir, S. E. Schacham, J. M. Garcia, and P. M. Petroff, Appl. Phys. Lett. **73**, 2003 (1998).
[9] S. J. Chua *et al.*, Appl. Phys. Lett. **73**, 1997 (1998).
[10] S. Sauvage, P. Boucaud, J.-M. Gérard, and V. Thierry-Mieg, J. Appl. Phys. **84**, 4356 (1998).
[11] S.-W. Lee, K. Hirakawa, and Y. Shimada, Appl. Phys. Lett. **75**, 1428 (1999).
[12] A. Weber, O. Gauthier-Lafaye, F. H. Julien, J. Brault, M. Gendry, Y. Désieres, and T. Benyattou, Appl. Phys. Lett. **74**, 413 (1999).
[13] H. Mohseni, E. Michel, J. Sandoen, M. Razeghi, W. Mitchel, and G. Brown, Appl. Phys. Lett. **71**, 1403 (1997).
[14] J. L. Liu, W. G. Wu, A. Balandin, G. L. Jin, and K. L. Wang, Appl. Phys. Lett. **74**, 185 (1999).
[15] J. L. Liu, W. G. Wu, A. Balandin, G. L. Jin, Y. H. Luo, S. G. Thomas, Y. Lu, and K. L. Wang, Appl. Phys. Lett. **75**, 1745 (1999).
[16] P. Boucaud, V. Le Thanh, S. Sauvage, D. Débarre, and D. Bouchier, Appl. Phys. Lett. **74**, 401 (1999).
[17] C. Miezner, O. Röthig, K. Brunner, and G. Abstreiter, Physica E (Amsterdam) **7**, 146 (2000).
[18] A. I. Yakimov, A. V. Dvurechenskii, Yu. Yu. Proskuryakov, A. I. Nikiforov, O. P. Pchelyakov, S. A. Teys, and A. K. Gutakovskii, Appl. Phys. Lett. **75**, 1413 (1999).
[19] M. A. Lampert and P. Mark, *Current Injection in Solids* (Academic, New York, 1970).
[20] A. I. Yakimov, A. V. Dvurechenskii, A. I. Nikiforov, and O. P. Pchelyakov, Phys. Low-Dimens. Semicond. Struct. **3/4**, 99 (1999).
[21] A. I. Yakimov, C. J. Adkins, R. Boucher, A. V. Dvurechenskii, A. I. Nikiforov, O. P. Pchelyakov, and G. Biskupskii, Phys. Rev. B **59**, 12 598 (1999).
[22] O. P. Pchelyakov, Yu. B. Bolhovityanov, A. V. Dvurechenskii, L. V. Sokolov, A. I. Nikiforov, A. I. Yakimov, and B. Voigtländer, Semiconductors **34**, 1229 (2000).
[23] B. F. Levine, J. Appl. Phys. **74**, R1 (1993).
[24] J. Tersoff, C. Teichert, and M. G. Lagally, Phys. Rev. Lett. **76**, 1675 (1996).
[25] Y. J. Mii, K. L. Wang, R. P. G. Karunasiri, and P. F. Yuh, Appl. Phys. Lett. **56**, 1046 (1990).
[26] A. Zussman, B. F. Levine, J. M. Kuo, and J. de Jong, J. Appl. Phys. **70**, 5101 (1991).
[27] B. F. Levine, A. Zussman, S. D. Ganapala, M. T. Asom, J. M. Kuo, and W. S. Hobson, J. Appl. Phys. **72**, 4429 (1992).
[28] *Optical and Infrared Detectors*, edited by R. J. Keyes (Springer, Berlin, 1980).
[29] A. I. Yakimov, A. V. Dvurechenski, N. P. Stepina, and A. I. Nikiforov, Phys. Rev. B **62**, 9939 (2000).
[30] R. P. G. Karunasiri, Y. J. Mii, and K. L. Wang, IEEE Electron Device Lett. **11**, 227 (1990).
[31] D. A. B. Miller, D. S. Chemla, T. C. Damen, A. C. Gossard, W. Wiegmann, T. H. Wood, and C. A. Burrus, Phys. Rev. B **32**, 1043 (1985).
[32] A. Harwit and J. S. Harris, Appl. Phys. Lett. **50**, 685 (1987).
[33] P. F. Yuh and K. L. Wang, J. Appl. Phys. **65**, 4377 (1989).
[34] Y. J. Mii, R. P. G. Karunasiri, K. L. Wang, M. Chen, and P. F. Yuh, Appl. Phys. Lett. **56**, 1986 (1990).
[35] For a review, see U. Meirav and E. B. Foxman, Semicond. Sci. Technol. **10**, 255 (1995).
[36] K. M. S. V. Bandara, D. D. Coon, B. O, Y. F. Lin, and M. H. Francombe, Appl. Phys. Lett. **53**, 1931 (1988).
[37] W. P. Chen, Y. J. Chen, and E. Burstein, Surf. Sci. **58**, 263 (1976).
[38] S. J. Allen, D. C. Tsui, and B. Vinter, Solid State Commun. **20**, 425 (1976).
[39] A. Pinczuk and J. M. Worlock, Solid State Commun. **36**, 43 (1980).
[40] T. Ando, Solid State Commun. **21**, 133 (1977).
[41] C. Metzner and G. H. Döhler, Phys. Rev. B **60**, 11 005 (1999).
[42] A. I. Yakimov, A. V. Dvurechenskii, V. V. Kirienko, Yu. I. Yakovlev, A. I. Nikiforov, and C. J. Adkins, Phys. Rev. B **61**, 10 868 (2000).
[43] M. Załużny, Phys. Rev. B **47**, 3995 (1993); J. Appl. Phys. **74**, 4716 (1993).
[44] K. Craig *et al.*, Phys. Rev. Lett. **76**, 2382 (1996).